



Preparation of cerium zinc oxide nanocomposite derived by hydrothermal route coated on glass and its application in water treatment

Mohammad Hossein Habibi*, Mosa Fakhrpor

Nanotechnology Laboratory, Department of Chemistry, University of Isfahan, Isfahan 81746-73441, I.R. Iran, Tel. +98 313 7934914; Fax: +98 313 6689732; emails: habibi@chem.ui.ac.ir (M.H. Habibi), mousafakhrpor1@gmail.com (M. Fakhrpor)

Received 4 February 2015; Accepted 1 March 2016

ABSTRACT

Ce and Zn oxide nanomaterials were effectively fabricated via one pot green and eco-friendly hydrothermal route. Ce and Zn oxide nanomaterials, terpineol, ethyl cellulose, and double distilled water were grinded and sonicated in four steps for improved coating. An efficient sonication route for improved coating of nanocomposite paste on glass for environmental application was investigated. Better dispersion of nanopaste by sonication for coating on glass was effective. The paste was deposited on the glass substrate through the Doctor Blade-coating and annealed in atmosphere at 550°C. The Ce and Zn oxide nanomaterials were characterized by thermo gravimetric analysis (TG-DTG), Fourier transform infrared, X-ray diffraction, field emission scanning electron microscopy, energy dispersive X-ray spectrometry, and UV–vis diffuse reflectance (DRS) spectroscopy techniques. Experimental studies for photocatalytic degradation of di-azo Naphthol Blue Black (NBB) textile dye from water systems revealed that Ce–Zn coupled oxide nanocomposite coated on glass was more effective in degradation of the dye compared with single Ce and Zn oxide nanomaterials.

Keywords: Nanopaste; Sonication; Sonocatalyst; Ce–Zn oxide; Nanomaterials; Di-azo; Naphthol Blue Black; Environmental

1. Introduction

Recently, much attention has been paid on the application of sono-chemical techniques for fabrication of nano-sized materials for their small size, uniform dispersion and high surface areas [1–6]. Among nano-sized materials, more efforts have been focused on the preparation of photocatalyst nanomaterials for their potential technological applications in environmental purposes. Among nanomaterials, more studies have

been performed on the nano-sized ZnO as an n-type semiconductor photocatalyst for its non toxicity, high stability, and low cost for degradation of environmental pollutants. Nano-sized ZnO has a wide direct band gap (E_g) of 3.37 eV which absorbs ultraviolet (UV) light for the degradation of environmental pollutants [7]. An important disadvantage for the practical use of nano-sized ZnO particles in treating waste water is the separation of these small size materials from water

*Corresponding author.

for recycling. Immobilization and coating the photocatalyst on to the surface of solid substrates has been an efficient method to solve the separation problem. Coating the photocatalyst paste on to the surface of solid substrates would have an excellent application for industrial production for its simple process and low cost [8]. Improving dispersion of nanoparticles in the paste by ultrasonication has been shown to be very effective [9]. Irradiation of nano-sized zinc oxide promotes an electron from valence band (VB) to conduction band (CB) leaving a hole in VB. Fast recombination of electrons and holes in zinc oxide as semiconductor and photocatalyst greatly reduces the efficiency of photocatalysis degradation. Coupling zinc oxide with another semiconductor oxide with different redox energy levels would increase the charge separation and decrease electron–hole recombination which results in efficiency of photocatalysis degradation [10–12]. Among metal oxide semiconductor photocatalysts, cerium oxide is the most active oxide catalyst in the rare earth oxide series and excellent material for photocatalytic applications [13–15]. Coupling cerium oxide with zinc oxide would result in the formation of composite mixed Ce–Zn oxide. Upon irradiation of composite mixed Ce–Zn oxide, the photo-generated electrons in the CB of cerium oxide travel to the CB of zinc oxide and photo-generated holes move from the VB of zinc oxide to the CB of cerium oxide rather than recombination of electron–hole [16–19].

In this research, we present a simple one pot green and eco-friendly hydrothermal route for the fabrication of Ce–Zn oxide nanomaterials using water as a green solvent. Characterization of Ce–Zn oxide nanomaterials was performed by TG-DTG, Fourier transform infrared (FT-IR), X-ray diffraction (XRD), field emission scanning electron microscopy (FESEM), Energy dispersive X-ray spectrometry (EDAX), and DRS. Ce–Zn oxide nanomaterials, terpineol, ethyl cellulose, and double distilled water were grinded and sonicated in four steps for better dispersion of nanomaterials in the paste matrix. The paste was coated on the glass using Doctor Blade-coating, annealed and applied for photocatalytic degradation of di-azo Naphthol Blue Black textile dye from water systems.

2. Materials and methods

2.1. Materials

Di-azo Naphthol Blue Black, ammonium cerium nitrate, $(\text{NH}_4)_2\text{Ce}(\text{NO}_3)_6$ (548.23 g/mol, 99% Merck Chemical), and Zinc nitrate as precursor $\text{Zn}(\text{NO}_3)_2 \cdot 6\text{H}_2\text{O}$ (297.47 g/mol, 99% Merck Chemical) were used without any purification.

2.2. Sono-catalyst preparation

2.2.1. Synthesis of Zn–Ce nanocomposite from zinc nitrate and ammonium cerium nitrate as precursors via hydrothermal method

Ammonium cerium nitrate, $(\text{NH}_4)_2\text{Ce}(\text{NO}_3)_6$, (3.323 g, 6 mmol) and zinc nitrate hexa-hydrate, $\text{Zn}(\text{NO}_3)_2 \cdot 6\text{H}_2\text{O}$, (1.803 g, 6 mmol) were dissolved in distilled water (20 mL) (0.3 mol L^{-1}). The pH value of the final reaction solution was adjusted to 9–10 by drop wise addition of ammonium hydroxide solution. Hydrothermal treatment was performed in a Teflon-lined stainless steel autoclave at 110°C for 12 h. Then the solution was filtered, washed several times with distilled water, and dried at 70°C with formation of phosphoric yellow powder (Fig. 1).

2.2.2. Sonication route for improved coating of nanocomposite paste on glass

Ce–Zn oxide nanomaterials (0.80 g) were grinded in a mortar and 130 μL of acetic acid was added and stirred at 5 min. Diluted water (130 μL) was added with stirring for one minute (5 times). Ethanol (130 μL) was added and stirred for one minute (15 times). Ethanol (300 μL) was added and stirred for one minute (6 times). All of the samples were sonicated for 3 min. Terpineol (0.8 mL) was added and the paste solution was sonicated for 3 min (3 times). The mixture was sonicated in an ultrasonic bath (Games, Model: Ultra 8060D-H, England) to achieve the homogeneity of Ce–Zn oxide nanomaterials. A solution of 0.4 g ethyl cellulose in 5 mL ethanol was stirred for 5 min and sonicated for 3 min and added to the reach of paste solution; then the all of solutions sonicated

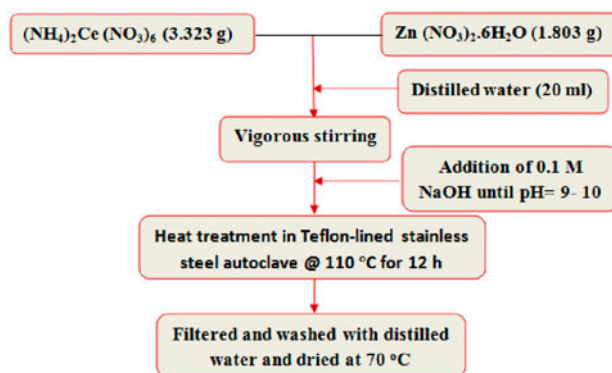


Fig. 1. Flow chart for the preparation of hetero-structured Zn–Ce oxide nanocomposite using ammonium cerium nitrate and zinc nitrate as precursors via hydrothermal method at 110°C for 12 h.

for 3 min (3 times). The solvent was evaporated in a rotary evaporator at r.t. Pastes of ZnO, CeO₂, and ZnO–CeO₂ nanomaterial were coated on a glass slide (6 cm × 2 cm and 2 μm thickness) separately by Doctor blade method and the thin films annealed at 550°C for 2 h (Fig. 2).

2.2.3. Photocatalytic application of sono-catalyst Ce–Zn oxide nanomaterials paste coated on glass by sonication route

Di-azo Naphthol Blue Black (NBB) textile dye solution as dye with a concentration of 20 ppm (calculated from the standard curve) and pH 3 was prepared as an initial solution and its absorbance was determined by Cary 500 UV–vis spectrophotometer at 620 nm. The dye solution was exposed to O₂ gas for 20 min. Thin films coated with nanoparticles photocatalyst were added separately into a Peti dish containing 20 mL contained 20 ppm of dye solution. The aqueous systems were magnetically stirred in the dark for 1 h to reach adsorption–desorption equilibrium of dye on the nanoparticles photocatalyst and then exposed to UV light. The irradiation distance between the lamp

and the sample was 8 cm. The reaction system was illuminated by a 250-W mercury lamp at different times and the concentration of the dye was determined by measuring the absorbance by UV–vis spectrophotometer at maximum absorption wavelength of 620 nm for photocatalytic activity examination.

2.3. Analytical methods

The mixtures were sonicated in an ultrasonic bath (Games, Model: Ultra 8060D-H, England) to achieve the homogeneity of Ce–Zn oxide nanomaterials. Pure Ce oxide, pure Zn oxide, and Ce/Zn nanostructures were each coated on borosilicate glass by Doctor Blade technique and spin coating method (Spin Coater, Modern Technology Development Institute, Iran). Ce–Zn oxide nanomaterials were characterized by X-ray diffractometer (D8 Advance, BRUKER). Band gap of cerium zinc oxide nanocomposite was determined using diffuse reflectance spectra (DRS) by a V-670 JASCO spectrophotometer and Munk relationship. The morphology of Ce–Zn oxide nanomaterials was analyzed by field emission scanning electron microscopy (FE-SEM, Hitachi, and model S-4160 at

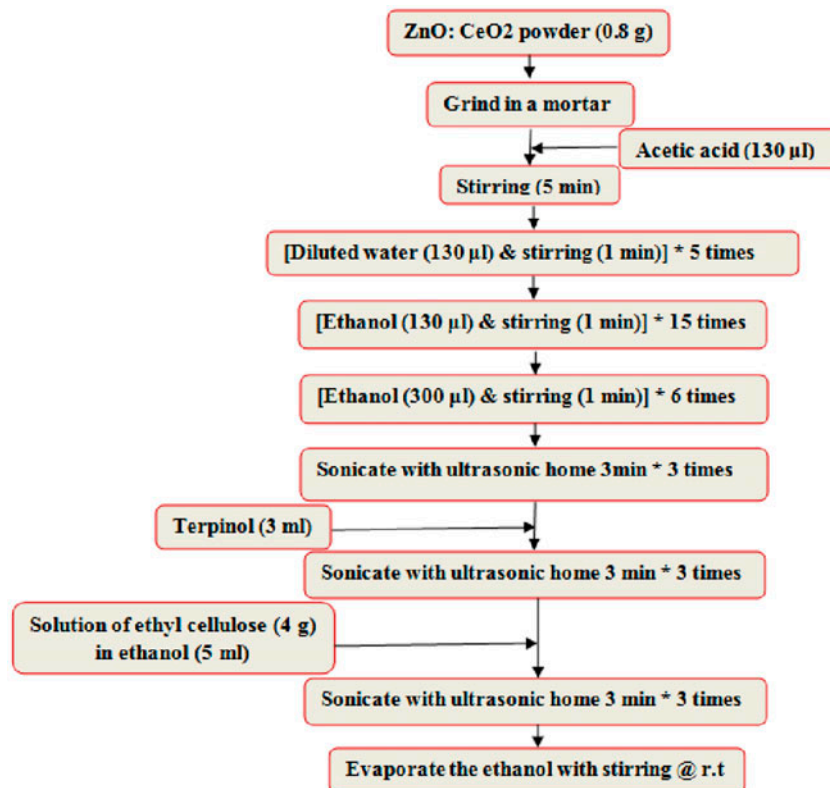


Fig. 2. Flow chart of sonication conditions for the preparation of hetero-structured Zn–Ce oxide nanocomposite paste for coating on glass by Doctor Blade.

100,000-time magnification). The chemical composition analysis of cerium zinc oxide nanocomposite was studied by energy-dispersive X-ray (EDXS) connected to the FE-SEM. A UV spectrophotometer (Varian Cary 500 Scan) was applied to analyze the pollutant dye concentrations. FT-IR absorption spectra of cerium zinc oxide nanocomposites were obtained using KBr disks on a JASCO FT-IR 6300.

3. Results and discussions

3.1. Sono-catalyst characterization

3.1.1. Structural study of sono-catalyst by FT-IR

FT-IR spectrum of Ce–Zn oxide nanocomposites synthesized from zinc nitrate and ammonium cerium nitrate via hydrothermal method dried at 70°C are shown in Fig. 3. The vibrational peak at 3,414 cm^{-1} is attributed to the hydroxyl group of water present in the solution. The peak at 1,383 cm^{-1} corresponds to the bending vibrational mode of the hydroxyl group. The bands in locations of 429, 505, 844, 1,063, 1,122, and 1,514 cm^{-1} are attributed to metal oxide M–O or M–O–M vibrations in binary zinc–cerium oxide (M = Zn or Ce). The results given by FT-IR analysis further confirm the formation of binary Ce–Zn oxide and thus support the XRD results.

3.1.2. Optical study by UV–vis absorption spectra (DRS)

The absorption spectra of single pure Ce and single pure Zn oxide nanostructures were presented for

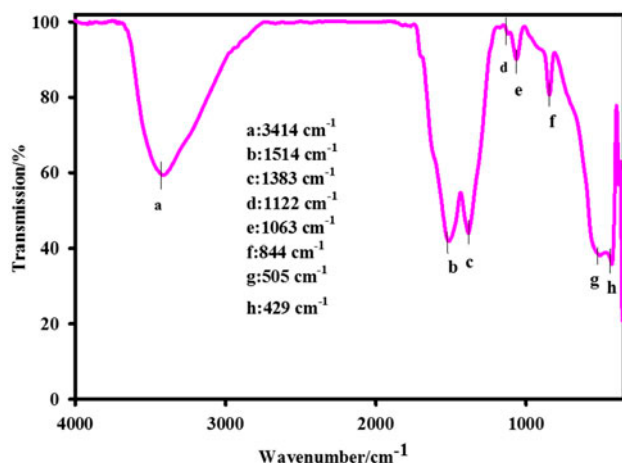


Fig. 3. FT-IR spectra of Zn–Ce oxide nanocomposite using ammonium cerium nitrate and zinc nitrate as precursors via hydrothermal method at 110°C for 12 h.

comparison with the hetero-structured Zn–Ce oxide nanocomposite. Zn–Ce coupled oxide nanocomposite showed the highest absorption coefficient in the UV region of 200–370 nm. The band gap energies of the photocatalyst given by Tauc plot are equal to 3.06, 2.85 and 2.27 eV and for pure ZnO, CeO₂, and ZnO–CeO₂ nanocomposite, respectively (Figs. 4a–4c). The results showed that the optical band gap energy of the Ce–Zn coupled oxide nanocomposites (2.27 eV) is much lower than that of pure Zn oxide nanoparticle (3.06 eV). The results showed that electron excitation in Ce–Zn coupled oxide nanocomposites occurs in the visible region ($\lambda = 546$ nm), while the electron excitation in pure Zn oxide nanoparticle occurs in the UV region ($\lambda = 405$ nm).

3.1.3. X-ray diffraction (XRD) study

The nanocomposite diffraction peaks matched the standard data for a hexagonal zinc Oxide ZnO (JCPDS 5-0664). The sample shows peaks attributed to the ZnO at 31.751 (1 0 0), 34.440 (0 0 2), 36.252 (1 0 1), 62.870 (1 0 3), 66,388 (2 0 0), 67.917 (1 1 2), 69.057 (2 0 1), and 81.405 (1 0 4), and for cubic cerium oxide CeO₂ (JCPDS 1-0,800). The sample shows peaks attributed to the CeO₂ at 28.550 (1 1 1), 47.485 (2 2 0), 56.343 (3 1 1), and 76.707 (3 3 1) (Fig. 5).

3.1.4. Morphological study by field emission scanning electron microscope (FESEM)

Fig. 6 shows the micrograph of Zn–Ce coupled oxide nanocomposite coated on glass after four steps

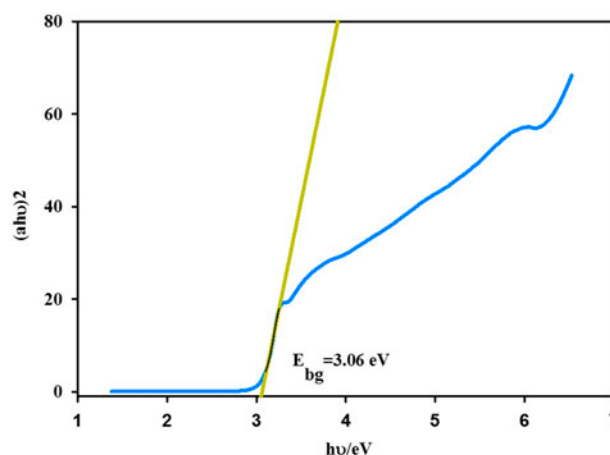


Fig. 4a. Tauc plot of pure single Zn oxide nano-particle using zinc nitrate as precursors via hydrothermal method.

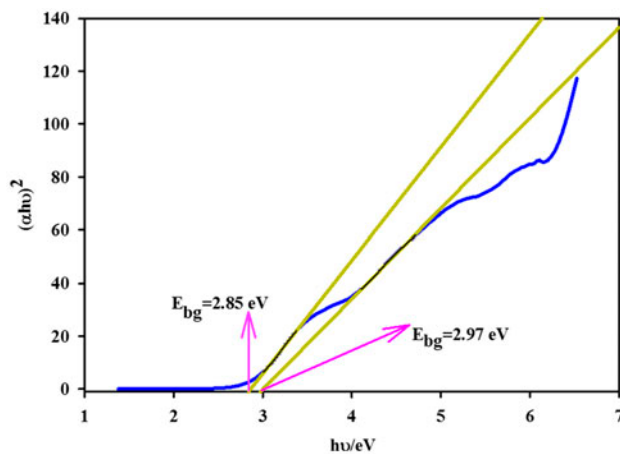


Fig. 4b. Tauk plot of pure single Ce oxide nano-particle using ammonium cerium nitrate as precursors via hydrothermal method.

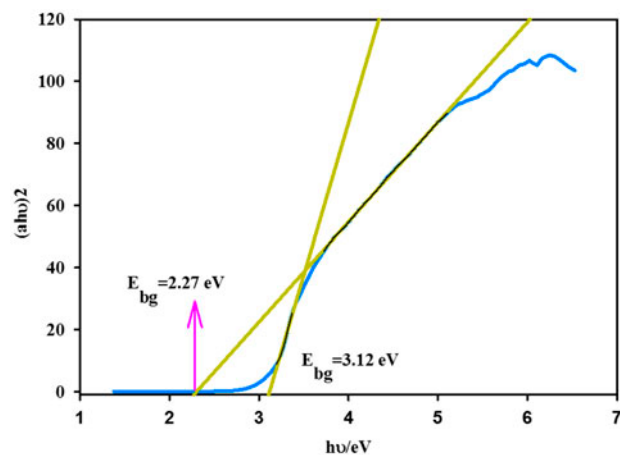


Fig. 4c. Tauk plot of Zn-Ce oxide nano-composite using ammonium cerium nitrate and zinc nitrate as precursors via hydrothermal method at 110°C for 12 h.

of sonication at 100,000 magnifications in 100 nm scale. It is clear from Fig. 7 that, the nanoparticles were well dispersed and similar types of particles in dispersion have been observed [20]. The nanoclusters formed among the particles in application of ultra-sonication process for better colloidal dispersion of nanofluid and the nanoclusters did not fully break down even after being exposed to prolonged ultra-sonication.

3.2. Compositional analysis of Zn-Ce coupled oxide nanocomposite coated on glass

Energy dispersive X-ray spectroscopy (EDX) analysis was carried out to analyze the composition of Zn-Ce coupled oxide nanocomposite coated on glass

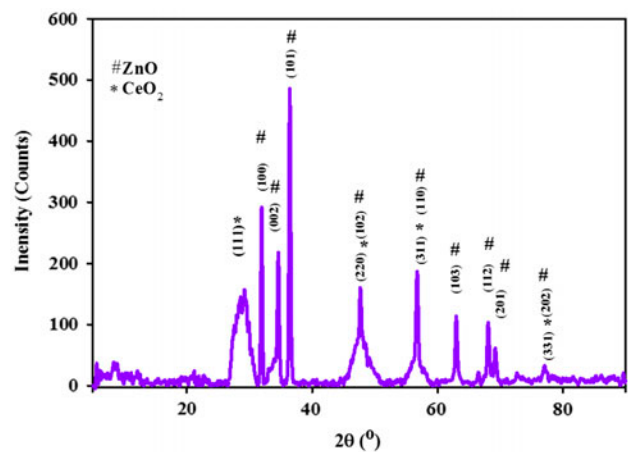


Fig. 5. XRD patterns of hetero-structured Zn-Ce oxide nanocomposite paste by ultra-sonication conditions coated on glass.

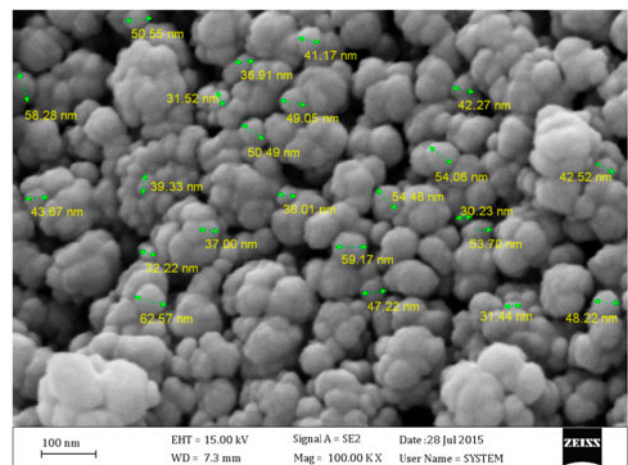


Fig. 6. FESEM images of hetero-structured Zn-Ce oxide nanocomposite paste at sonication conditions coated on glass.

after four steps of sonication. The EDX spectra of these oxides are shown in Fig. 7 and the results showed peaks corresponding to Zn, Ce. The results of EDX analysis are in agreement with XRD data.

3.3. Photocatalytic degradation and mechanism

The photocatalytic activity of single pure Ce oxide, single pure Zn oxide nanostructures, and hetero-structured Zn-Ce oxide nanocomposite was characterized by the degradation test of di-azo Naphthol Blue Black (NBB) textile dye in water systems. The changes in the absorption spectra of di-azo Naphthol Blue Black exposed to irradiation for various irradiation times (0, 20, 40, 60, 80, 100, and 120 min) in the

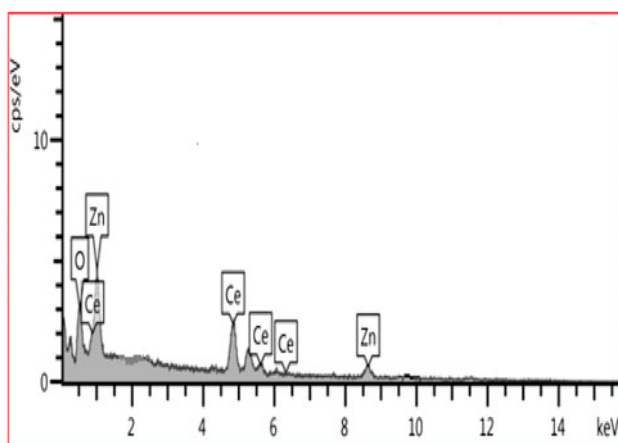


Fig. 7. EDX spectra of hetero-structured Zn–Ce oxide nanocomposite paste at sonication conditions coated on glass.

presence of single pure Ce oxide, single pure Zn oxide nanostructures, and hetero-structured Zn–Ce oxide nanocomposite coated on glass are shown in Fig. 8. The absorption maxima at 620 and 650 nm decreased gradually with the extension of irradiation time. As can be seen in Fig. 9, the photocatalytic activity of hetero-structured Zn–Ce oxide nanocomposite is much higher than single pure Ce oxide, single pure Zn oxide nanostructures. The superior photocatalytic activity of hetero-structured Zn–Ce oxide nanocomposite Ce can be attributed to the inter particle electron and hole transfer between cerium oxide and zinc oxide and thus the delayed recombination of photo-excited electron-hole pairs. When Zn oxide is coupled with Ce oxide, it forms n–n type

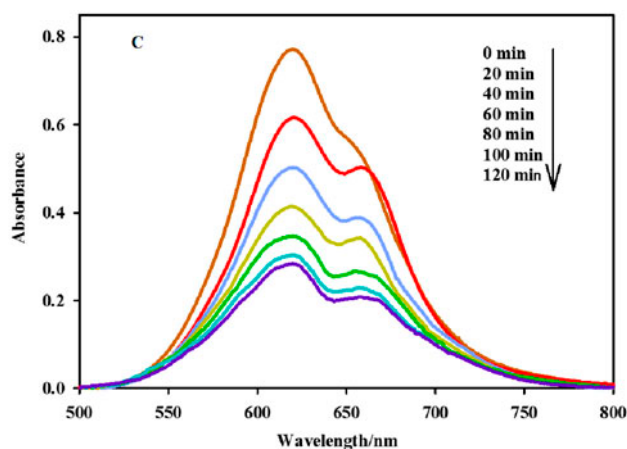


Fig. 8. The change in absorption spectra of di-azo Naphthol Blue Black exposed to irradiation for various irradiation times (0, 20, 40, 60, 80, 100, and 120 min) in the presence of hetero-structured Zn–Ce oxide nanocomposite coated on glass.

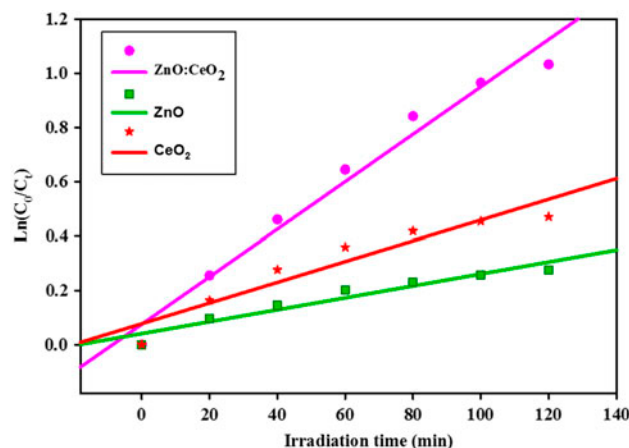


Fig. 9. $\ln(C_0/C_t)$ vs. time (min) (first-order reaction) for the photocatalytic degradation of di-azo Naphthol Blue Black exposed to irradiation for various irradiation times (0, 20, 40, 60, 80, 100, and 120 min) in the presence of single pure Ce oxide, single pure Zn oxide nanostructures, and hetero-structured Zn–Ce oxide nanocomposite coated on glass.

heterojunction. In such junction electron transfer can occur from semiconductor with low work function (CeO_2) to the other with high work function (ZnO) until the Fermi levels equalize. This creates an electron depleted layer at the interface of ZnO and CeO_2 which bends the energy band. The enhanced photocatalytic performance of composite CeO_2 – ZnO is attributed to the combined effect of the formation of depleted layer at the surface of CeO_2 – ZnO , hence lower electron–hole recombination and better charge separation. Moreover, the optical band gap energy of the Ce–Zn coupled oxide nanocomposites (2.27 eV) is much lower than that of pure Zn oxide nanoparticle (3.06 eV) and electron excitation in Ce–Zn coupled oxide nanocomposites occurs at visible region ($\lambda = 546$ nm), while the electron excitation in pure Zn oxide nanoparticle occurs at UV region ($\lambda = 405$ nm). The photocatalytic degradation of di-azo Naphthol Blue Black (NBB) textile dye in water systems in the presence of single pure Ce oxide, single pure Zn oxide, and hetero-structured Zn–Ce oxide nanocomposite coated on glass follows the pseudo-first-order kinetics (Fig. 9) and it can be expressed as follows: $\ln(C_0/C) = kt$, where C_0 is the initial concentration of Naphthol Blue Black at $t = 0$ min, C , the concentration of Naphthol Blue Black at irradiation time t and k is the rate constant [21,22].

4. Conclusions

In summary, Ce and Zn oxide nanomaterials were fabricated via hydrothermal route, grinded, and

sonicated in four steps for improved coating. An efficient sonication route for improved coating of nanocomposite paste on glass for environmental application was investigated. Better dispersion of nanopaste by sonication for coating on glass was effective. The paste was deposited on the glass substrate through the Doctor Blade-coating and annealed in atmosphere at 550°C. The Ce and Zn oxide nano-sized sono-catalysts were characterized by FT-IR, XRD, FESEM, EDAX, and DRS spectroscopy techniques. Experimental studies for photocatalytic degradation of di-azo Naphthol Blue Black (NBB) textile dye from water systems revealed that Ce–Zn coupled oxide nanocomposite paste sonicated in four steps coated on glass was more effective in degradation of the dye compared with single Ce and Zn oxide nanomaterials.

Acknowledgment

The authors wish to thank the University of Isfahan for financially supporting this work.

References

- [1] M.A. Behnajady, B. Alizade, Enhancement of TiO₂-UV100 nanoparticles photocatalytic activity by Mg impregnation in the removal of a model organic pollutant, *Desalin. Water Treat.* 53(3) (2015) 689–696.
- [2] X. Guo, Q. Wei, B. Du, Y. Zhang, X. Xin, L. Yan, H. Yu, Removal of basic dyes (malachite green) from aqueous medium by adsorption onto amino functionalized graphenes in batch mode, *Desalin. Water Treat.* 53(3) (2015) 818–825.
- [3] M. Sheibani, M. Ghaedi, F. Marahel, A. Ansari, Congo red removal using oxidized multiwalled carbon nanotubes: Kinetic and isotherm study, *Desalin. Water Treat.* 53 (2015) 844–852.
- [4] F. Marahel, M.A. Khan, E. Marahel, I. Bayesti, S. Hosseini, Kinetics, thermodynamics, and isotherm studies for the adsorption of BR2 dye onto avocado integument, *Desalin. Water Treat.* 53(3) (2015) 826–835.
- [5] N.K. Singh, S. Saha, A. Pal, Solar light-induced photocatalytic degradation of methyl red in an aqueous suspension of commercial ZnO: A green approach, *Desalin. Water Treat.* 53(2) (2015) 501–514.
- [6] R.M. Mohamed, E.S. Aazam, Enhancement of photocatalytic activity of ZnO–SiO₂ by nano-sized Ag for visible photocatalytic reduction of Hg(II), *Desalin. Water Treat.* 50(1–3) (2012) 140–146.
- [7] H. Daraei, A. Maleki, A.H. Mahvi, Y. Zandsalimi, L. Alaei, F. Gharibi, Synthesis of ZnO nano-sono-catalyst for degradation of reactive dye focusing on energy consumption: Operational parameters influence, modeling, and optimization, *Desalin. Water Treat.* 52 (2014) 6745–6755.
- [8] A.M. Badawi, S.M. Ahmed, S.A. Shaban, S.M.I. Morsy, Nanotechnology: The next revolution for wastewater treatment (TNT contaminate), *Desalin. Water Treat.* 40 (1–3) (2012) 1–6.
- [9] D. Chakraborty, S.S. Gupta, Decolourisation of Metanil Yellow by visible-light photocatalysis with N-doped TiO₂ nanoparticles: Influence of system parameters and kinetic study, *Desalin. Water Treat.* 52 (2014) 5528–5540.
- [10] A. Nezamzadeh-Ejhieh, Z. Banan, Photodegradation of dimethylsulfide by heterogeneous catalysis using nano CdS and nano CdO embedded on the zeolite A synthesized from waste porcelain, *Desalin. Water Treat.* 52 (2014) 3328–3337.
- [11] M. Inagaki, Y. Nakazawa, M. Hirano, Y. Kobayashi, M. Toyoda, Preparation of stable anatase-type TiO₂ and its photocatalytic performance, *Int. J. Inorg. Mater.* 3 (2001) 809–811.
- [12] M.H. Habibi, M. Zendehtdel, Synthesis and characterization of titania nanoparticles on the surface of microporous perlite using sol–gel method: Influence of titania precursor on characteristics, *J. Inorg. Organomet. Polym. Mater.* 21 (2011) 634–639.
- [13] M.H. Habibi, M. Zendehtdel, Fabrication and characterization of self-assembled multilayer nanostructure titania with high preferential (101) orientation on alumina thin films by layer-by-layer dip-coating method, *Curr. Nanosci.* 6 (2010) 642–647.
- [14] D.S. Bhatkhande, V.G. Pangarkar, A.A. Beenackers, Photocatalytic degradation for environmental applications: A review, *J. Chem. Technol. Biotechnol.* 77 (2001) 102–116.
- [15] M.P. Reddy, A. Venugopal, M. Subrahmanyam, Hydroxyapatite-supported Ag–TiO₂ as *Escherichia coli* disinfection photocatalyst, *Water Res.* 41 (2007) 379–386.
- [16] X. Wang, S.O. Pehkonen, A.K. Ray, Removal of aqueous Cr(VI) by a combination of photocatalytic reduction and coprecipitation, *Ind. Eng. Chem. Res.* 43(7) (2004) 1665–1672.
- [17] M.H. Habibi, N. Talebian, J.-H. Choi, The effect of annealing on photocatalytic properties of nanostructured titanium dioxide thin films, *Dyes Pigm.* 73(1) (2007) 103–110.
- [18] M.H. Habibi, R. Mokhtari, Novel sulfur-doped niobium pentoxide nanoparticles: Fabrication, characterization, visible light sensitization and redox charge transfer study, *J. Sol–Gel Sci. Technol.* 59 (2011) 352–357.
- [19] J. Tang, J.R. Durrant, D.R. Klug, Mechanism of photocatalytic water splitting in TiO₂. Reaction of water with photoholes, importance of charge carrier dynamics, and Evidence for four-hole chemistry, *J. Am. Chem. Soc.* 130 (2008) 13885–13891.
- [20] M.H. Habibi, M. Mikhak, Synthesis of nanocrystalline zinc titanate eandrewsite by Sol–Gel: Optimization of heat treatment condition for red shift sensitization, *Curr. Nanosci.* 7 (2011) 603–607.
- [21] M.H. Habibi, I. Farsani, Enhanced photocatalytic degradation of C.I. reactive orange 86 in aqueous environment using nanostructure Zn_{1–x}Co_xO composite thin film coated on glass, *Desalin. Water Treat.* 22 (2010) 204–210.
- [22] M. Nasr-Esfahani, M.H. Habibi, A comparative study on physicochemical properties and photocatalytic behavior of two different nanostructure composite TiO₂ films coated on glass substrate, *Desalin. Water Treat.* 3 (2009) 64–72.